Mapping Protein Interfaces with a Fluorogenic Cross-Linker and Mass Spectrometry: Application to Nebulin−Calmodulin Complexes

ARTICLE *in* BIOCHEMISTRY · AUGUST 2001

Impact Factor: 3.02 · DOI: 10.1021/bi010259+ · Source: PubMed

2 AUTHORS, INCLUDING:

Andrea Sinz
Martin Luther University Halle-Wittenberg
124 PUBLICATIONS **2,433** CITATIONS

SEE PROFILE

Mapping Protein Interfaces with a Fluorogenic Cross-Linker and Mass Spectrometry: Application to Nebulin−Calmodulin Complexes

Andrea Sinz‡ and Kuan Wang*

Laboratory of Physical Biology, National Institute of Arthritis and Musculoskeletal and Skin Diseases, National Institutes of Health, Bethesda, Maryland 20892

Received February 6, 2001; Revised Manuscript Received March 16, 2001

ABSTRACT: Nebulin is a giant multifunctional protein that is thought to serve as both a length-regulating protein ruler and calcium/CaM-mediated regulatory protein on the thin filaments of the skeletal muscle sarcomere. To define molecular interfaces between nebulin and CaM, we thiolated lysines of CaM and ND66, a four-module cloned fragment from the C-terminus of nebulin, with 2-iminothiolane and cross-linked the complex with dibromobimane, which alkylates thiol pairs within ∼6 Å of each other to form a fluorescent adduct. Such a two-stage cross-linking generated mainly 1:1 complexes of ND66 and CaM, with a limited extent of intramolecular cross-linking. In-gel chymotryptic digestion of the dibromobimane-cross-linked complexes yielded peptides that were first screened by HPLC with fluorescence detection and then scored for cross-linking with mass spectrometry. Several inter- and intramolecular sites were identified and confirmed further by ESI-MS/MS experiments, defining molecular interfaces and patterns of protein folding. In particular, five intermolecular cross-linking products of sequences within the region of amino acids 83−99 (YKENMGKGTPLPVTPEM) in ND66 and several sequences of CaM indicate that the nebulin−CaM interface is close to, and may overlap with, the nebulin−actin interface. This proximity suggests a potential competition between CaM and actin for this nebulin interface. Intramolecular cross-linking of amino acids 13−16 (KEAF) and 13−18 (KEAFSL) with amino acids 145−148 (MTAK) and 146−148 (TAK) in CaM suggests the interaction of two lobes across the central helix. The cross-linking of amino acids 1−6 (MKTPEM) with amino acids 114−129 (YKENVGKATATPVTPE) and 115−129 (KENVGKATATPVTPE) in ND66 hints at an association of noncontiguous nebulin modules in solution.

Recent thrusts in proteomics emphasize the global cataloging of all expressed proteins in normal and diseased tissues. A systematic identification of molecular interfaces between interacting proteins in their natural cellular environment represents the next major challenge in proteomics. Protein interactions are now routinely identified or inferred from the protein connectivity maps based on phage display or yeast two-hybrid screening techniques (*1*). Whether any such interactions manifest themselves in situ, however, remains open. Chemical cross-linking, a conceptually attractive approach for profiling protein interfaces in their cellular environment, has been applied with success to the identification of nearest neighbors, e.g., of membrane proteins in intact erythrocytes (*2*). Identification of cross-linked sequences and amino acids has until now been hampered by a lack of suitable techniques for resolving and identifying the vast number of cross-linked products. Current developments of mass spectrometry in resolving and identifying complex biomolecular mixtures have greatly enhanced the potential of this unique approach in delineating details of protein interfaces in situ.

The feasibility of applying chemical cross-linking combined with mass spectrometry to identify sequences at the interfaces is demonstrated in recent investigations of the inter- or intramolecular contact regions between monomers of the homodimeric DNA binding protein ParR (*3*), between glycoproteins CD28 and CD80 (*3*), and components of the Nup84p complex from the yeast nuclear pore (*4*).

We recently proposed the use of fluorogenic cross-linkers, in combination with HPLC and MALDI-MS analysis, as a step toward improving the efficiency and throughput of cross-linking analysis (*5*). The production of fluorescent products allows the fractionation and purification of cross-linked peptides, thus enhancing the confidence of the subsequent mass spectrometric analysis. As a first step to illustrate the feasibility of this approach, we are applying dibromobimane (DB),[1] a fluorogenic thiol specific cross-linker (*6*), to elucidate the protein interfaces between ND66, a C-terminal cloned fragment of the giant muscle protein nebulin, and CaM.

Nebulin, originally identified as band 3 of myofibrillar proteins (*7*), comprises 2−3% of the myofibrillar protein of skeletal muscle and displays tissue and developmentally specific isoforms in the range of 600−900 kDa (*8*−*10*). The nebulin gene has been located to chromosome 2q24.1−24.2,

* To whom correspondence should be addressed: Building 6, Rm. 401, Laboratory of Physical Biology, National Institute of Arthritis and Musculoskeletal and Skin Diseases, NIH, Bethesda, MD 20892. Phone: (301) 496-4097. Fax: (301) 402-8566. E-mail: wangk@exchange.nih.gov.

‡ Present address: Proteome Center Rostock, Medical Faculty, University of Rostock, Joachim-Jungius-Str. 9, D-18059 Rostock, Germany.

10.1021/bi010259+
Published on Web 06/09/2001

and mutations in the nebulin gene have been linked to the typical or "mainstream" autosomal recessive nemaline myopathy (*11*, *12*). Recently, an invertebrate nebulin was identified in the cross-striated body muscle of the lancelet (*13*). Immunoelectron microscopy indicates that a single nebulin molecule spans the whole length of the thin filament, with its C-terminus anchored in the Z-line and its N-terminus extending toward the distal end of the thin filament (*8*, *9*, *14*).

Analysis of the deduced protein sequence and structural motifs of human nebulin from adult (*15*) and fetal (*16*) skeletal muscles reveals the design principles of this giant multifunctional protein in the sarcomere. The bulk of nebulin, between the unique N- and C-terminal sequences, is constructed of about 200 tandem repeats of an approximately 35-residue module, which can be further organized into super-repeats, with each super-repeat containing seven modules. In contrast, both the SH3 domain containing the C-terminal region anchored in the Z-line and the N-terminus of nebulin form unique sequences. Synthetic nebulin modules (*17*) and recombinant nebulin fragments containing 2−15 modules (*16*, *18*−*20*) all bind actin, and most of them bind CaM, tropomyosin, and troponin (*16*). Nebulin fragments from the N-terminal half of the molecule situated in the actomyosin overlap region of the sarcomere inhibit actomyosin ATPase activities, as well as sliding velocities of actin over immobilized myosin as shown by in vitro motility assays (*21*). CaM reverses the nebulin fragments' inhibition of ATPase and accelerates actin sliding in the presence of high calcium concentrations. In contrast, an actin-binding nebulin fragment (ND66) derived from the single-repeat region at the C-terminus binds to CaM, but does not bind to myosin or prevent actin from sliding (*21*). The C-terminal nebulin modules are thus unlikely to play a regulatory role in the actomyosin interaction. To understand the structural basis of the nebulin−CaM interaction, we sought to define the molecular interfaces between nebulin and CaM. For this purpose, the four-module nebulin fragment ND66 was selected as a representative of these single-repeat modules that binds to both actin and CaM, but not to myosin.

MATERIALS AND METHODS

Expression and Purification of Cloned Calmodulin. Permanent cultures of pEx1-CaM/JM109 (DE3) (chicken CaM) were a generous gift from T. C. Squier (University of Kansas, Lawrence, KS). The cultures were inoculated into 20 mL of LB broth containing tetracyclin (8 μg/mL) and incubated at 37 °C while being shaken at 200 rpm overnight. To obtain a sufficient amount of cells to induce the required amount of CaM expression, 20 mL of the overnight culture was transferred into 2 L of LB broth containing tetracyclin (8 μg/mL) and incubated at 37 °C until the OD_{600} reached a value of 0.3−0.4 (∼3 h) before IPTG was added. The cells were incubated for an additional ∼5 h, and harvested by centrifugation at 6000 rpm. Cell pellets were resuspended in 30 mL of buffer containing 50 mM Tris-HCl, 2 mM Na-EDTA, and 1 mM DTT (pH 7.4). The samples were then treated three times with a French press at 1000 psi. The cytosol was separated from cell debris by centrifugation at 19 500 rpm for 20 min, leaving expressed CaM in the supernatant. CaM was purified using a hydrophobic column essentially as described previously (*22*) and was further purified using weak anion exchange HPLC as described previously (*23*). Protein concentrations were determined by absorbance at 280 nm (A_{280} = 0.2 for 1 mg/mL).

Expression and Purification of Cloned Nebulin Fragment ND66. ND66 was expressed and purified as described previously (*24*). Protein concentrations were determined by absorbance at 280 nm (A_{280} = 0.355 for 1 mg/mL).

EDC Cross-Linking of ND66 with CaM. A mixture of ND66 and CaM [45 μM each in 5 mM Tes-Na (pH 7.6), 1 mM Na-EDTA, and 2 mM $CaCl_2$] was treated with different mixtures of EDC and s-NHS (5 mM each, 10 and 5 mM, and 20 and 5 mM) at 23 °C. Aliquots (50 μL) were taken at 1, 4, 15, and 30 min, and the reaction was quenched with DTT (40 mM).

DB Cross-Linking of ND66 with CaM. (1) Reactivity of DB with Reaction Buffer. Five microliters of a DB solution (100 mg/mL in acetonitrile) was incubated at 40 °C overnight with 200 μL of 20 mg/mL Tes-Na (pH 7.6). The reaction products were analyzed by ESI-MS (see below).

(2) Thiolation and Cross-Linking. ND66 and CaM [2 mg/mL in 50 mM sodium phosphate buffer (pH 8.0)] were treated separately with a freshly prepared stock solution (2 mg/mL) of 2-iminothiolane (methyl 4-mercaptobutyrimidate; Pierce Chemical Co., Rockford, IL) to give a molar ratio (reagent:protein) of 10 and reacted for 1 h at 23 °C. The thiolated proteins were separated from unreacted 2-iminothiolane with a spin column of Sephadex G-25 medium (Amersham Pharmacia Biotech AB, Uppsala, Sweden), collected in 5 mM Tes-Na and 1 mM Na-EDTA (pH 7.6) in a final volume of 100 μL, and used immediately for cross-linking reactions. The degree of modification was calculated from the mass increase (Δm = 102.2 per MBA moiety) in MALDI-MS. Thiolated ND66 (100 μL, 120 μM) and thiolated CaM (100 μL, 120 μM) were mixed with 200 μL of 5 mM Tes-Na, 1 mM Na-EDTA, and 2 mM $CaCl_2$ (pH 7.6, pCa 3.0) and treated with 150 μM (6 μL of a 10 mM stock in acetonitrile) DB ("Thiolyte DB", Calbiochem, La Jolla, CA) for 25 min at 23 °C in the dark. DTT was added to a final concentration of 40 mM to quench the reaction.

Gel Electrophoresis and In-Gel Digestion. The reaction mixture was solubilized in $^1/_2$ volume of Laemmli sample buffer [50 mM Tris-HCl, 2% SDS, 10% glycerol, 30 mg/mL pyronin Y, and 18.5 mg/mL DTT (pH 6.8)] and boiled for 2 min. Electrophoresis (∼70 μg of protein per lane) was carried out at room temperature in a Tricine-SDS gradient gel system (4 to 20%, Novex, San Diego, CA). The gel was imaged with a Kodak CF440 Imaging Station with a 450 nm cutoff long-pass filter (Thin Film Technologies, Inc., Greenfield, MA) to detect DB-containing proteins (emission

[1] Abbreviations: CaM, calmodulin; DB, 4,6-bis(bromomethyl)-3,7-dimethyl-1,5-diazabicyclo[3.3.0]octa-3,6-diene-2,8-dione (dibromobimane); DTT, dithiothreitol; EDC, 1-ethyl-3-[3-(dimethylamino)propyl]-carbodiimide; EDTA, ethylenediaminetetraacetic acid; ESI-MS, electrospray ionization mass spectrometry; HCCA, α-cyano-4-hydroxycinnamic acid; HPLC, high-performance liquid chromatography; IPTG, isopropyl β-D-thiogalactopyranoside; LB, Luria-Bertani medium; MALDI-TOF MS, matrix-assisted laser desorption ionization time-of-flight mass spectrometry; MBA, mercaptobutyramidine; nESI-MS, nano electrospray ionization mass spectrometry; SDS−PAGE, sodium dodecyl sulfate−polyacrylamide gel electrophoresis; s-NHS, *N*-hydroxysulfosuccinimide; Tes-Na, tris(hydroxymethyl)methyl-2-aminoethanesulfonic acid, sodium salt; TFA, trifluoroacetic acid; Tris, tris(hydroxymethyl)-aminomethane.

maximum $\lambda = 477$ nm, excitation at $\lambda = 385$ nm). After imaging, the gel was stained with Coomassie Blue.

The fluorescent bands corresponding to the ND66−CaM (1:1) complexes (band II, ~16 μg of protein) as well as the monomer bands of CaM and ND66 (band I, ~15 μg of protein) from the same lane were cut out with a scalpel, chopped into pieces (volume of ~0.5−1.0 mm^3), and collected in 1.5 μL brown plastic tubes. A piece of gel of similar size was also cut from the blank region and treated in parallel. The gel pieces were washed once with 150 μL of water, twice with 150 μL of a 50% acetonitrile/50% water mixture, and once with 80 μL of acetonitrile, 80 μL of 100 mM NH_4HCO_3, and 80 μL of acetonitrile. The gel particles were dried (Speed-vac SC110 apparatus, Savant Instruments Inc., Holbrook, NY) before chymotrypsin sequencing grade (Boehringer Mannheim, Indianapolis, IN) in 2 μg in 20 μL of 100 mM Tris and 10 mM $CaCl_2$ (pH 7.8) was added to the samples and the control. After 5 min, 20 μL of 100 mM Tris and 10 mM $CaCl_2$ was added to cover the gel pieces completely. At the end of the digestion (25 °C for 16 h), the peptide digests were collected by washing gel pieces four times with 50 μL of a 50% acetonitrile/50% water/5% TFA mixture. The pooled supernatants were lyophilized and redissolved in 80 μL of water.

Reversed Phase HPLC. Each of the digests (80 μL) was injected into a HP1100 HPLC system (Agilent Technologies, Palo Alto, CA) equipped with a photodiode array UV detector and a fluorescence detector. A C-18 Jupiter column (250 mm × 2.0 mm, 5 μm, 300 Å, Phenomenex, Torrance, CA) was equilibrated with 2% A (A being an 80% acetonitrile/20% water mixture with 0.052% TFA) before sample application. The peptides were eluted at 200 μL/min using the following gradient: 98 to 62.5% B from 0 to 60 min, 62.5 to 37.5% B from 60 to 90 min, 37.5 to 2% B from 90 to 105 min (B being water and 0.06% TFA). Fractions were monitored by both absorption at 220 nm and fluorescence at 477 nm (excited at 385 nm). The fractions were dried and dissolved in 25 μL of water and stored at −20 °C before MALDI-MS analysis.

MALDI-TOF MS. Peptide digests for mass spectrometry were prepared by mixing 1 μL of a sample solution with 4 μL of a saturated matrix solution [recrystallized α-cyano-4-hydroxycinnamic acid (HCCA) (Fluka, Milwaukee, WI) in 30% acetonitrile, 70% water, and 0.1% TFA] and spotting 1.3 μL onto a stainless steel target. The mixture was air-dried before insertion into a MALDI time-of-flight mass spectrometer (Proflex III, Bruker Daltonics, Billerica, MA), equipped with a nitrogen laser (337 nm) and operated in reflectron mode. Spectra were obtained by summation of 50−70 laser shots. ACTH(18−39) ($[M+H]^+_{mono} = 2465.20$), substance P ($[M + H]^+_{mono} = 1347.74$), and bombesin ($[M + H]^+_{mono} = 1691.82$) were used as external calibrants. A database search for chymotryptic peptides was performed using the SwissProt Database (http://www.expasy.ch). For protein analysis, sinapinic acid (Sigma, St. Louis, MO) in 30% acetonitrile, 70% water, and 0.1% TFA was used as the matrix, and the mass spectrometer was operated in the linear mode. Horse heart myoglobin ($[M + H]^+ = 16\,952$), cytochrome *c* ($[M + H]^+ = 12\,361$), and bovine serum albumin ($[M + H]^+ = 66\,431$) were used as external calibrants.

ESI-MS. Sample solutions were diluted 1:2 with a MeOH/0.1% CH_3COOH mixture (1:1) and introduced into the ESI ion trap mass spectrometer (Esquire-LC, Bruker Daltonics) with a syringe pump (Cole-Parmer, Niles, IL) at a flow rate of 2 μL/min. All measurements were conducted in the positive ionization mode at a capillary voltage of −4000 V with a dry gas temperature of 250 °C. Eight spectra were averaged to one profile mass spectrum.

NanoESI-MS/MS. All spectra were obtained on an Esquire-LC system (Bruker Daltonics) equipped with a NanoSpray source and conducted in the positive ionization mode (on-voltage of 600 V) using a 1.0 Da width isolation window, with He as the collision gas.

Scoring Cross-Linked Peptides by NIH-XL. MALDI mass spectra were analyzed to identify cross-linked peptides with the aid of in-house software (NIH-XL). NIH-XL assigns each mass signal as either an unmodified peptide or a modified peptide. For each modified peptide, it then calculates linear combinations of molecular weights of two peptides, each with a range of thiolations at lysines, and a number of DB modifications. The user provides a list of peptides and their molecular weights based on the known cleavage sites of the enzyme and protein sequences from the database. In the paper presented here, incomplete cleavages (up to three sites) and "unwanted" cleavages by trypsin contamination (on lysines and arginines) were also taken into consideration in generating the final peptide listings. 2-Iminothiolane was assumed to react exclusively with lysine residues, causing a mass increase of 102.2 units per reacted lysine. Up to three lysines per peptide were assumed to be modified. The cross-linking reagent DB causes a mass shift of 187.2 units, taking into account the fact that peptide masses are obtained from the database as protonated species.

The present version of NIH-XL does not yet consider any side reactions of DB, such as hydrolysis, in scoring the peptides, which has to be done manually.

An outline of our experimental strategy for the determination of interaction sites between CaM and ND66 is depicted in Figure 1.

RESULTS

Cross-Linking with EDC. The four-module nebulin fragment ND66, derived from the C-terminal single-repeat region of human fetal nebulin, interacts with CaM with a binding constant in the micromolar range (K. Linse and K. Wang, unpublished data). To identify the residues involved in the cross-linking, we have initially explored the analysis with a zero-length cross-linker that has been successful in elucidating the binding sites of nebulin with actin (*25*) and myosin (O. Andreev and K. Wang, manuscript submitted for publication).

As shown in Figure 2, a broad band of 1:1 complexes at ~31 kDa is formed with a high yield (~33%) following treatment of an ND66/CaM (1:1) mixture with EDC and s-NHS for 1 min. The large width of this band may be caused by the formation of multiple cross-linking products, both inter- and intramolecular, that are poorly resolved in SDS gels. The extensive intramolecular cross-linking of CaM by EDC and s-NHS is evident by the formation of the faster migrating smear below CaM before significant 1:1 complexes with ND66 are formed. Cross-linking of ND66 and CaM at

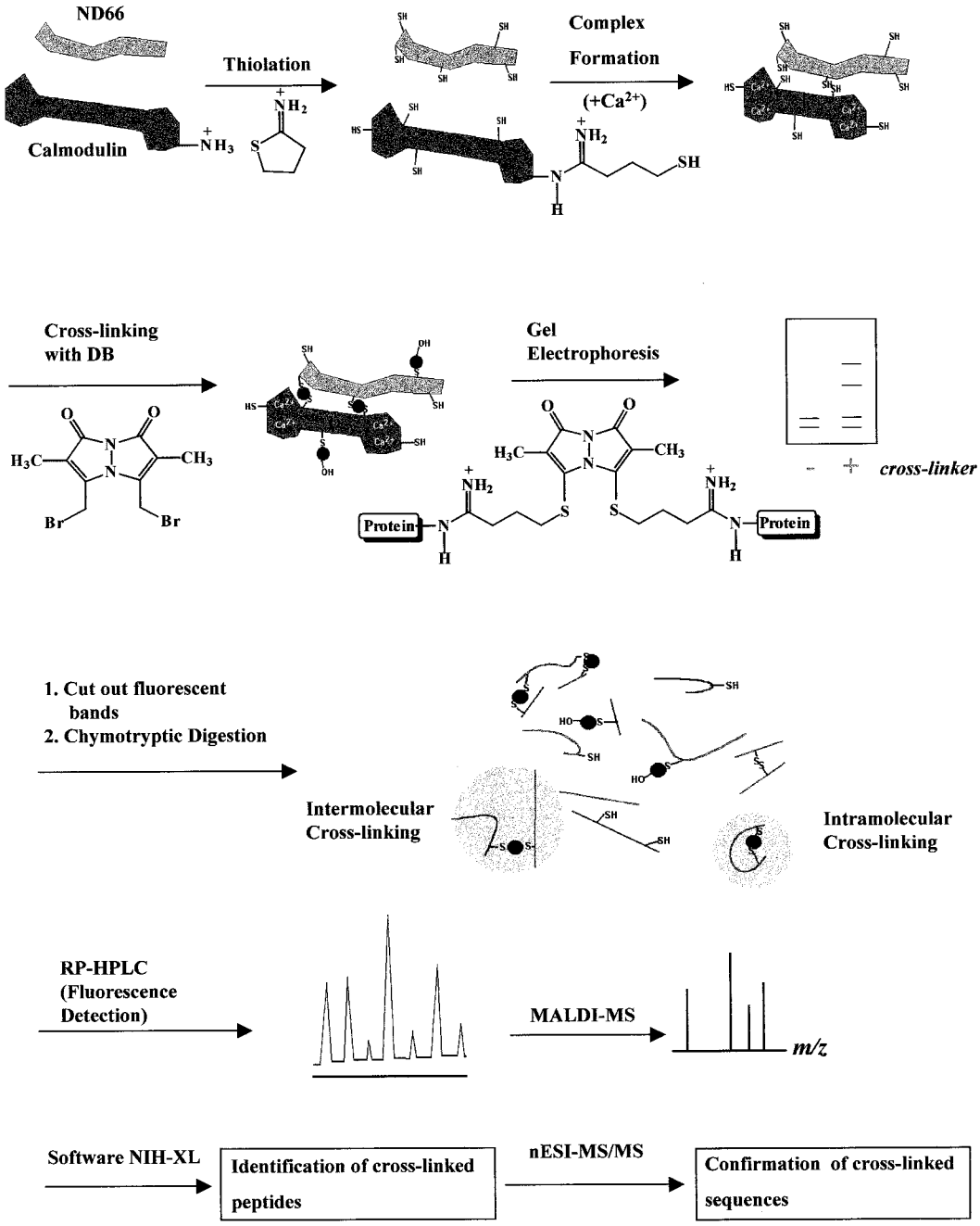

FIGURE 1: Identification of protein interfaces with a fluorogenic cross-linker and mass spectrometry.

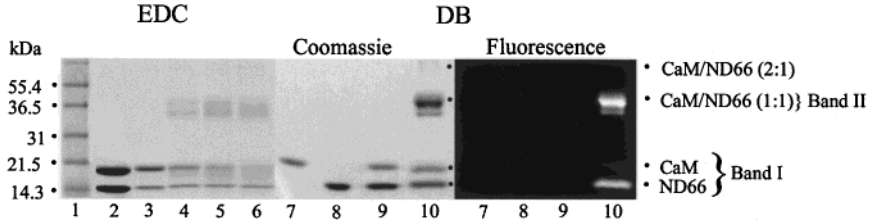

FIGURE 2: Cross-linking of CaM and ND66 via treatment with EDC and s-NHS and DB at pCa 3.0. EDC cross-linking. A mixture of CaM (45 μM) and ND66 (45 μM) was cross-linked for 1 min at room temperature in 5 mM Tes buffer (with 1 mM Na-EDTA) at pCa 3.0 with EDC and s-NHS at several molar ratios: lane 1, markers; lane 2, CaM and ND66; lane 3, CaM/ND66 mixture (1:1) without EDC or s-NHS; lane 4, CaM/ND66 mixture (1:1) with 5 mM EDC and 5 mM s-NHS; lane 5, CaM/ND66 mixture (1:1) with 10 mM EDC and 5 mM s-NHS; lane 6, CaM/ND66 mixture (1:1) with 20 mM EDC and 5 mM s-NHS. DB cross-linking. A mixture of thiolated CaM (30 μM) and ND66 (30 μM) was cross-linked with 150 μM DB for 25 min at room temperature in 5 mM Tes-Na and 1 mM Na-EDTA (pH 7.6, pCa 3.0): lane 7, CaM; lane 8, ND66; lane 9, CaM and ND66, thiolated; lane 10, CaM/ND66 mixture (1:1) with a 5-fold molar excess DB. Coomassie Blue staining and fluorescence imaged with a Kodak Imager 440 CF instrument (450 nm long-pass filter).

several molar ratios (1:2, 2:1, and 3:1) with EDC and s-NHS resulted in the exclusive formation of 1:1 complexes (data not shown). Cross-linking of ND66 and CaM with EDC and s-NHS at high and low calcium concentrations (pCa 4 and

8) yielded 1:1 complexes in both cases, indicating that the interaction does not require calcium. However, since the sites of interactions are yet to be mapped, the possibility that this interaction is calcium-dependent is still open (A. Sinz and K. Wang, unpublished data).

Efforts made to minimize intramolecular cross-linking by a two-stage cross-linking reaction (activating ND66 with EDC and s-NHS before adding CaM) did not result in products of intermolecular cross-linking (data not shown). We therefore focused our attention on the two-stage method with the fluorogenic cross-linker DB that alkylates thiols within ~6 Å.

Cross-Linking with DB. Neither CaM nor ND66 contains cysteine residues for alkylation by DB, so it was necessary to thiolate both proteins before the cross-linking reaction. The reagent that we used, 2-iminothiolane, specifically modifies primary amines to form mercaptobutyramidines (MBAs) that retain the intrinsic charge of lysines, and therefore, the conformation of the proteins is expected to differ little from that of the native proteins. The extent of thiolation, as checked by MALDI-MS analysis with a mass shift of 102.2 units for each MBA moiety introduced, was one to two SH residues per CaM and five to eight SH residues per ND66.

The cross-linking reaction of ND66 and CaM with DB was conducted in low-concentration Tes-Na buffer (5 mM) at pH 7.6 in the presence of 1 mM Ca^{2+} as shown in Figure 2. Unreacted DB is essentially nonfluorescent, but after replacement of both bromines, it becomes fluorescent, exhibiting an emission maximum at 477 nm after excitation at 385 nm. As a result, cross-linked products containing reacted DB can be easily detected by their fluorescence at 477 nm. Fluorescence detection of unstained gels immediately revealed a significant degree of cross-linking in monomers of ND66 and CaM as well as the formation of 1:1 complexes and some higher-molecular weight complexes (Figure 2). It is noted that with two-stage cross-linking, there is relatively little intramolecular cross-linking within CaM, as indicated by the sharp CaM band in contrast to the smearing of EDC-treated CaM. This protocol also led to sharper bands of cross-linked complexes. There was no evidence of dimer bands of either ND66 or CaM resulting from cross-linking during transient collisions of nonassociated proteins in solution.

MALDI mass spectra (Figure 3) of the same reaction mixtures used for gel electrophoresis showed signals for ND66 at *m*/*z* 15 050, 15 228, and 15 318 (monomeric ND66, with a range of modifications by MBA and/or DB), as well as signals for CaM at *m*/*z* 16 910 and 17 099 (monomeric CaM, with a range of modifications by MBA and/or DB). The doubly charged signals of both monomers are also evident in the spectrum (asterisks in Figure 3). A broad signal from *m*/*z* 33 090 to 33 795 corresponds to different CaM−ND66 (1:1) complexes with different amounts of MBA and/or DB introduced. Another broad signal from *m*/*z* 50 689 to 53 280 was assigned as 2:1 CaM−ND66 complexes, with the same modifications for both proteins. A weak signal from *m*/*z* 65 972 to 71 227 corresponds to 2:2 CaM−ND66 complexes at low yield. Again, no cross-linked dimers of CaM or ND66 were detected by mass spectrometry.

Scoring for Cross-Linked Peptides by NIH-XL. The fluorescent bands corresponding to the 1:1 ND66−CaM complexes (band II) and monomeric ND66 and CaM bands (band I) from the same lane (lane 10, Figure 2) were excised and in-gel digested with chymotrypsin that produced peptides with masses between 800 and 3500 Da for MALDI analysis (Figure 4).

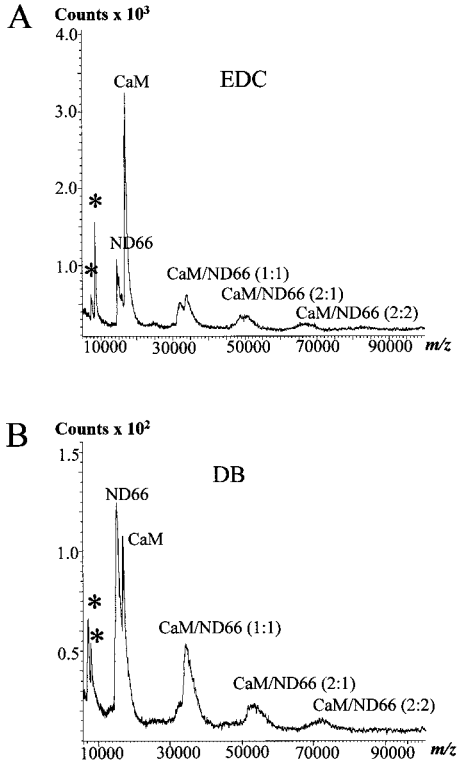

FIGURE 3: MALDI mass spectra of EDC- and DB-cross-linked mixtures. The same samples that were used for gel analysis as in Figure 2 (lanes 4 and 10) were analyzed by MALDI-MS. Asterisks indicate doubly charged molecular ions of CaM and ND66.

The chymotryptic digests were separated by reversed phase HPLC using dual detection with UV at 220 nm and fluorescence at 477 nm. A comparison of this pair of elution profiles reveals that DB-containing peptides elute over a narrow range of retention times between 26 and 56 min. These fluorescent HPLC fractions were subjected to MALDI-MS analysis and scored for evidence of inter- and intramolecular cross-linking with NIH-XL.

It was clear that these mixtures would be complex, even after enrichment by selecting fluorescence-containing fractions. A large percentage of the peptides are derived from unmodified CaM and ND66 sequences, and a few peptides can be assigned to autolyzed chymotrypsin. These signals, as well as signals from the digestion of a blank gel piece, are excluded from further considerations. To simplify analysis of the remaining data, we have limited ourselves to scoring candidates for peptides containing only a binary complex and excluded any that may contain three or more peptide sequences. The scoring by mass analysis requires detailed knowledge of the reaction and its products. DB is thought to react specifically with sulfhydryl groups (*6*). However, since other nucleophilic substitution reactions of DB with the reaction buffer might occur, we evaluated its side reactions experimentally by incubating DB at 40 °C overnight with Tes-Na buffer and the reaction mixture was subsequently analyzed along with unreacted DB by ESI-MS (Figure 5). Commercial DB is slightly contaminated with

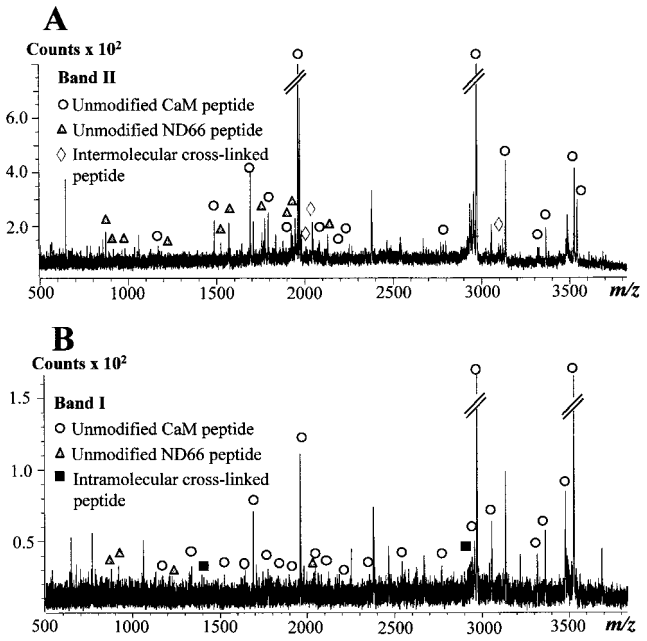

FIGURE 4: MALDI mass spectra from one of four unfractionated chymotryptic digests for band I and band II. Band II (1:1 complexes) (A) and band I (ND66 and CaM, un-cross-linked) (B) were in-gel digested with chymotrypsin and analyzed by MALDI-MS. Signals were scored with NIH-XL. From this digest of band II, three intermolecular cross-linking products of CaM and ND66 were identified (A) after fractionation of the mixture by HPLC (Figure 6). Also, two intramolecular cross-linking products, one from CaM and one from ND66, were identified from this digest of band I (B).

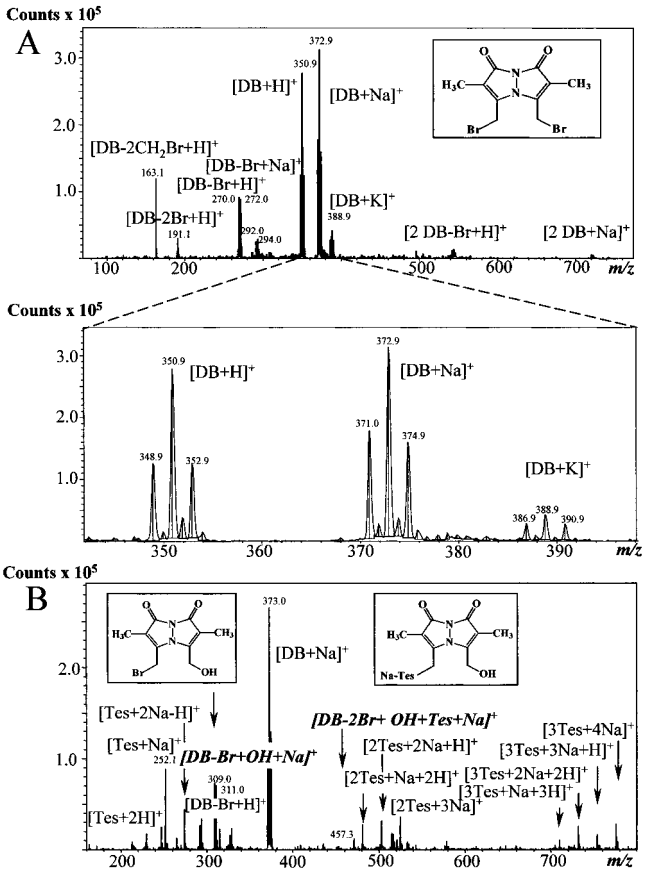

FIGURE 5: Reactions of DB with buffer components. (A) ESI-MS of unreacted DB. Bromine atoms in DB display easily recognized isotopic patterns (signal ratios of 1:1 for one Br and 1:2:1 for two Br; $\Delta m = 2$ units). The inset shows the formula of DB. (B) ESI-MS of DB incubated with Tes-Na at 40 °C for 12 h. The main reaction is water hydrolysis of DB. The reaction product [DB − 2Br + OH + Tes + Na]$^+$ at *m/z* 457.3 is formed only to a minor extent. No signals for [DB − 2Br + 2Tes + H/Na]$^+$ are detectable. The insets show the partial hydrolysis product of DB and the reaction product of DB with water and Tes-Na.

monobromobimane ([M + H]$^+$ *m/z* 270.0 and 272.0, 1:1 intensities) and bimane ([M + H]$^+$ *m/z* 191.0). After incubation with buffer components, the major reaction appears to be the hydrolysis of DB, as indicated by the presence of signals at *m/z* 309.0 and 311.0, with 1:1 intensities, corresponding to [DB − Br + OH + Na]$^+$. Only a negligible amount of reaction product between Tes-Na and DB was detected, even after reaction at 40 °C overnight. These experiments indicate that only the monosubstituted hydrolysis product of DB needs to be taken into consideration in the scoring of cross-linked peptides by computation and side reactions with other nucleophiles are negligible under the reaction conditions of low buffer concentration and short reaction time.

Table 1: Intermolecular Cross-Linking Products of CaM and ND66[a]

observed [M + H]$^+$	calculated [M + H]$^+$	peptide	chymotryptic fragment	peptide sequence	no. of MBAs	no. of DBs
2123.4	*2123.4**	*a*	88−99 (ND66)	GKGTPLPVTPEM	1	1
	(F19+20)	A	73−76 (CaM)	ARKM	1	
3264.6	*3264.9*	*b*	83−99 (ND66)	YKENMGKGTPLPVTPEM	1	1
	(F24)	B	69−76 (CaM)	LTMMARKM	1	
1844.6	1844.1	*c*	83−87 (ND66)	YKENM	1	1
		C	93−99 (CaM)	DKDGNGY	1	
3354.2	3353.9	*c*	83−87 (ND66)	YKENM	1	1
		D	90−109 (CaM)	RVFDKDGNGYISAAELRHVM	1	
3029.8	3030.9	*d*	84−99 (ND66)	KENMGKGTPLPVTPEM	2	1
		E	142−148 (CaM)	VQMMTAK	1	
2032.8	*2033.3**	*e*	1−7 (ND66)	MKTPEMM	1	1
	(F13)	F	110−116 (CaM)	TNLGEKL	1	

[a] Sequence of ND66: [1]MKTPEMMRVKQTQDHISSVKYKEAIGQGTPIPDLPEVKRVKETQKHISSV[51]MYKENLGTGIPTTVTPEIERVKRNQENFSSVLYKENMGKGTPLPVTPEME[101]RVKHNQENISSVLYKENVGKATATPVTPE. Sequence of CaM: [1]ADQLTEEQIAEFKEAFSLFDKDGDGTITTKELGTVMRSLGQNPTEAELQD[51]MINEVDADGNGTIDFPEFLTMMARKMKDTDSEEEIREAFRVFDKDGNGYI[101]SAAELRHVMTNLGEKLTDEEVDEMIREADIDGDGQVNYEEFVQMMTAK. Cross-linked products were identified from four digests of 1:1 complexes (band II). Signals for 1:1 cross-linked peptides show a mass increase of 2 × 102.2 units (2× MBA modification) + 187.2 units (DB − 2Br; 1H was subtracted, as the peptide list from the SwissProt database, which was used as input in NIH-XL, gives [M + H]$^+$ values). Calculations were carried out with the NIH-XL software package. Italicized values are for cross-linked peptides identified from fluorescent HPLC fractions (Figure 6). Asterisks indicate cross-linked peptides that were confirmed by nESI-MS/MS experiments.

Table 2: Intramolecular Cross-Linking Products of CaM and ND66[a]

observed $[M + H]^+$	calculated $[M + H]^+$	peptide	chymotryptic fragment	peptide sequence	no. of MBAs	no. of DBs
1336.0	1336.0	G	13−16 (CaM)	KEAF	1	1
		H	145−148 (CaM)	MTAK	1	
1405.2	1405.1	I	13−18 (CaM)	KEAFSL	1	1
		J	146−148 (CaM)	TAK	1	
2669.2	2669.8	K	19−32 (CaM)	FDKDGDGTITTKEL	2	1
		L	72−76 (CaM)	MARKM	1	
2927.5	2927.9	M	17−32 (CaM)	SLFDKGDGTITTKEL	2	1
		I	13−18 (CaM)	KEAFSL	1	
3096.4	3096.8	N	1−18 (CaM)	ADQLTEEQIAEFKEAFSL	1	1
		L	72−76 (CaM)	MARKM	1	
3120.3	3119.9	O	90−109 (CaM)	RVFDKDGNGYISAAELRHVM	1	1
		H	145−148 (CaM)	MTAK	1	
2770.1	2771.9	*g*	115−129 (ND66)	KENVGKATATPVTPE	2	1
		f	1−6 (ND66)	MKTPEM	1	
2935.1	2934.9	*h*	114−129 (ND66)	YKENVGKATATPVTPE	2	1
		f	1−6 (ND66)	MKTPEM	1	
3399.2	3399.0	*i*	57−78 (ND66)	GTGIPTTVTPEIERVKRNQENF	1	1
		j	84−87 (ND66)	KENM	1	
3562.9	3562.1	*i*	57−78 (ND66)	GTGIPTTVTPEIERVKRNQENF	1	1
		k	83−87 (ND66)	YKENM	1	

[a] Cross-linked products identified from four digests of a mixture of monomeric ND66 and calmodulin (band I). Signals of cross-linked peptides show a mass increase of 2 × 102.2 units (2× MBA modification) + 187.2 units (DB − 2Br; 1H was subtracted, as the peptide list from the SwissProt database, which was used as input in NIH-XL, gives $[M + H]^+$ values). The calculation was carried out with the NIH-XL software package.

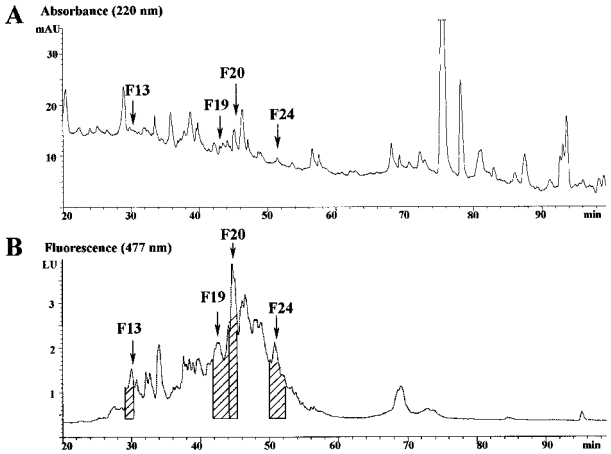

FIGURE 6: Reversed phase HPLC of chymotryptic digests of 1:1 complexes (band II). The same digest of 1:1 complexes that was used for MALDI-MS analysis in Figure 4A was applied to reversed phase HPLC with UV (A) and fluorescence (B) dual detection. The UV elution profile (A) indicates that major peptides in the digest are well-resolved. However, the fluorescence profile (B) shows that fluorescent cross-linked peptides are minor components and elute early with partial resolution. All fluorescent fractions were collected and analyzed by MALDI-MS and the NIH-XL software package.

With the proper user input for scoring peptides for cross-linking, we have identified several candidates for inter- and intramolecular cross-linking (Tables 1 and 2). Analysis of several fluorescent fractions is described in detail below. It is useful to emphasize that scoring by the NIH-XL software is based solely on the molecular weight of potential cross-linked peptides. All candidate sequences are listed when they meet the criterion that the total mass is accounted for by the summation of the individual mass of the component peptides, the monofunctional derivative, and the cross-linker. Unambiguous identification of the cross-linked peptides thus requires further sequence analysis, such as ESI-MS/MS experiments. This process is illustrated below with two fractions from one out of the four totally performed digests of band II.

F13. Fraction 13 in the fluorescence chromatogram (Figure 6) contained a signal with a $[M + H]^+$ at *m*/*z* 2033.8 that had been identified as a cross-linked product of residues 1−7 (MKTPEMM) of ND66 and residues 110−116 (TNLGEKL) of CaM (Figure 8A and Table 1). A signal at *m*/*z* 1017.1, corresponding to the doubly charged molecular ion, yielded a tandem mass spectrum showing a signal at *m*/*z* 787.4 (Figure 7A). This signal corresponds to the doubly charged ion of a cross-linking product of the y_6 ion of residues 1−7 of ND66 and the y_4 ion of residues 110−116 of CaM (thiolated). A signal at *m*/*z* 770.6 corresponds to a doubly charged ion of cross-linking products of the b_5 ion of residues 1−7 of ND66 (thiolated) with the y_5 ion of residues 110−116 of CaM (thiolated). The scoring with the NIH-XL software was confirmed by nESI-MS/MS experiments.

F19+20. Fraction 19 and 20 in the fluorescence chromatogram (Figure 6) contained a signal with a $[M + H]^+$ at *m*/*z* 2123.4 that had been identified as a cross-linked product of residues 88−99 of ND66 and residues 73−76 of CaM (Figure 8A and Table 1). nESI-MS/MS analysis of a signal at *m*/*z* 1062.4, corresponding to the doubly charged molecular ion, yielded a fragmentation spectrum (Figure 7B) showing as a base peak a signal at *m*/*z* 948.9. This signal corresponds to the doubly charged ion of a cross-linking product of residues 88−99 (GKGTPLPVTPEM) of ND66 (with K89 thiolated), cross-linked with DB to the y_2 ion of residues 73−76 (ARKM) of CaM (with K75 thiolated). This is further confirmed by the observation of a signal at *m*/*z* 940.4, corresponding to the z_2 ion of residues 73−76 (ARKM) of CaM (with K75 thiolated), cross-linked with residues 88−99 of ND66. Another signal at *m*/*z* 912.1 could be assigned to the doubly charged ion of a cross-linking product of the b_{11} ion of residues 88−99 of ND66 (thiolated) and the b_3 ion of residues 73−76 of CaM (thiolated). nESI-MS/MS analysis thus confirms the identification based on initial scoring with NIH-XL.

We noted that the fragmentation patterns of cross-linked peptides were complex and not yet useful for sequencing

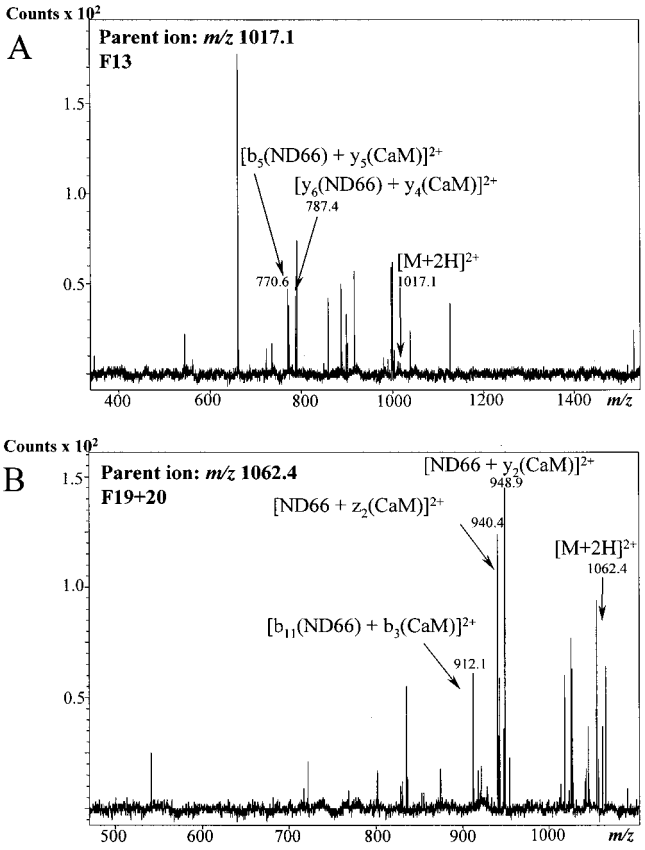

FIGURE 7: nESI-MS/MS of selected signals for cross-linked peptides. (A) Fragmentation pattern of a signal at *m*/*z* 1017.1 corresponding to $[M + 2H]^{2+}$ (HPLC F13, Figure 6) of a cross-linking product of ND66 (amino acids 1−7, peptide *e*, Table 1 and Figure 8A) and CaM (amino acids 110−116, peptide F, Table 1 and Figure 8A). (B) Fragmentation pattern of a signal at *m*/*z* 1062.4 corresponding to $[M + 2H]^{2+}$ (HPLC F19+20, Figure 6) of a cross-linking product of ND66 (amino acids 88−99, peptide *a*, Table 1 and Figure 8A) and CaM (amino acids 73−76, peptide A, Table 1 and Figure 8A). Fragment ions in mass spectrometry are commonly referenced by the Biemann nomenclature (38). b ions are derived from cleavage of the peptide bond, with the charge located on the N-terminal fragment, and y ions are derived from cleavage of the peptide bond, with the charge located on the C-terminal fragment. The number indicates the amino acid residue where cleavage occurs.

the peptide components. Further work is clearly necessary to evaluate how derivatization influences the fragmentation of these peptides.

Molecular Interfaces between ND66 and CaM. MALDI-MS analysis of the chymotryptic digests revealed many underivatized fragments from both of the proteins, giving more than 90% sequence coverage for ND66 and ∼30% sequence coverage for CaM. It is striking that the cross-linked peptides between both proteins point to two distinct regions in the ND66 sequence (Figure 8A and Table 1). Five of six possible cross-linking products are derived from residues 83−99 (YKENMGKGTPLPVTPEM, peptides *a*−*d*), and only one cross-linked peptide is derived from the N-terminus (residues 1−7, peptide *e*) of ND66. For CaM, several loci are involved. Two possible cross-linking products contain residues 69−76 (LTMMARKM, peptide B) and residues 73−76 (ARKM, peptide A), respectively, that are located in the central α-helix of CaM; two cross-linked peptides are derived from residues 90−109 (RVFDKDGNYISAAELRHVM, peptide D) and residues 93−99 (DKDGNGY, peptide C) that are located in the EF-hand of CaM, and one cross-linked peptide each is derived from residues 110−116 (TNLGEKL, peptide F) and residues 142−148 (VQMMTAK, peptide E) that represent the C-terminus of CaM.

The fact that the vast majority of cross-linking products for ND66 are located in the region of amino acids 83−99 suggests that this region is at or near the molecular interfaces with CaM in the complexes. Since the 1:1 complexes obviously consist of multiple bands that were poorly resolved in SDS gels and MALDI mass spectra (Figures 2 and 3), it is likely that not all identified cross-linking sites are present in all complexes.

Intramolecular Cross-Linking. Mass spectrometric analysis of monomeric, fluorescent CaM and ND66 (band I) yielded useful information about intramolecular cross-linking and protein folding patterns (Figure 8B and Table 2). For ND66, principally two intramolecular cross-linking products were observed: one from residues 114/115−129 to residues 1−6 (peptides *h*/*g* and *f*), thus connecting the C-terminus with the N-terminus of ND66; and another from residues 57−78 to residues 83/84−87 (peptides *i* and *k*/*j*), bringing two nebulin modules together. For CaM, six potential intramolecular cross-linking products were identified by NIH-XL. Two cross-linking products, from residues 13−16 to residues 145−148 (peptides G and H) and from residues 13−18 to residues 146−148 (peptides I and J), indicate that the two lobes of CaM can be cross-linked across the central helix under our experimental conditions. Two products, from residues 19−32 to residues 72−76 (peptides K and L) and from residues 1−18 to residues 72−76 (peptides N and L), cross-link the N-terminal region with the central helix of CaM. Two further products, from residues 17−32 to residues 13−18 (peptides M and I) and from residues 90−109 to residues 145−148 (peptides O and H), cross-link sequences within the same lobes.

To ease the comparison with known conformations of CaM, inter-residue contacts of CaM residues in two conformational states are presented as off-diagonal spots above and below the diagonal line of the two-dimensional plots (Figure 9). The contacts based on X-ray crystallography (Protein Data Bank entry 1CLL) and NMR (Protein Data Bank entry 1CFC) are represented as squares, and those determined by our DB cross-linking data are represented as spots superimposed on both contact maps. It is useful to bear in mind that (1) the "contact" distance in cross-linking is operationally defined by the size and span of the reagents and the flexibility of the lysine side chains. Therefore, diagonal boxes are minimal estimates of spacing, and (2) it is nearly impossible to draw definitive conclusions about protein interactions or proximity from the absence of cross-linking. The contact map here thus represents a "minimum" map, with the caveat that the absence of off-diagonal squares does not necessarily indicate the absence of contacts.

DISCUSSION

Molecular Interfaces by Chemical Cross-Linking. This study has demonstrated that by a proper combination and integration of fluorogenic cross-linking, enrichment by HPLC, and identification of cross-linked peptides by mass spectrometry and computation, valuable information about molecular interfaces can be defined or implicated. From

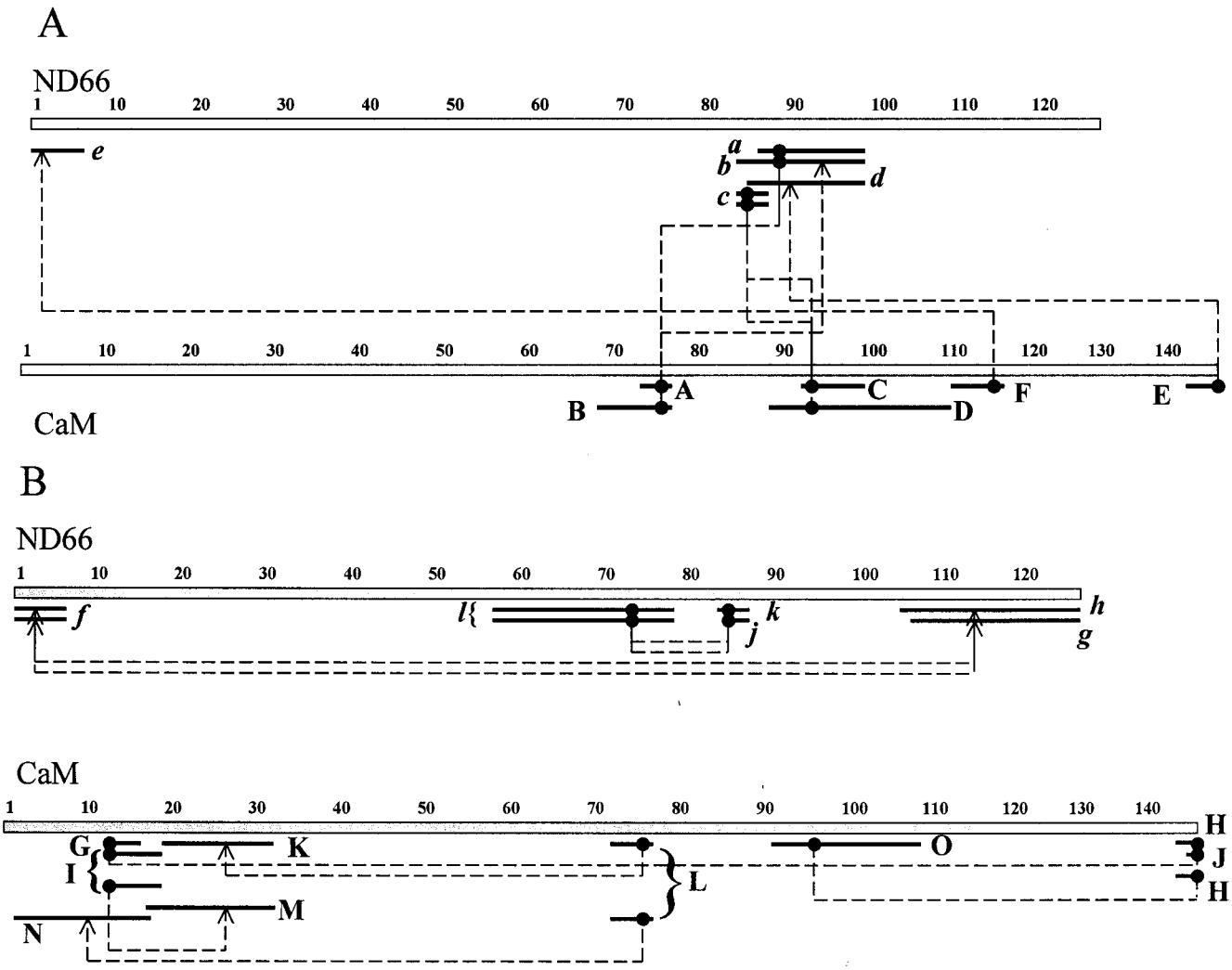

FIGURE 8: Intermolecular and intramolecular cross-linking sites. (A) Intermolecular cross-linking sites between ND66 and CaM. (B) Intramolecular cross-linking sites of ND66 and CaM. Peptides are designated as in Tables 1 and 2. Balls indicate that the exact cross-linking residue is known; arrowheads indicate that the cross-linking residue is uncertain.

intermolecular cross-linking sites, one can define sites of interaction. From intramolecular cross-linking sites, one can deduce rudimentary folding patterns. Rapid recent development of mass spectrometry in resolution, sensitivity, and mass range is likely to greatly facilitate the challenging task of cataloging molecular interfaces by chemical cross-linking. As illustrated here, future comprehensive cataloging of cross-linking sites will require detailed knowledge of the chemistry of the cross-linkers with the proteins being studied. It also demands highly specific cleavage methods, techniques for enriching cross-linked peptides, high-resolution mass spectrometers, and rapid computational techniques for scoring the massive amount of mass spectrometric data, and sequence confirmation by ESI-MS/MS or other techniques.

Nebulin and CaM Interface. CaM binds with a broad range of affinities (from nanomolar to micromolar) and broad specificity to basic amphiphilic α-helical peptides (Baa helices) found in many CaM-binding proteins (*26*). The interaction of ND66 and CaM is of low affinity with a binding constant in the micromolar range (K. Linse and K. Wang, unpublished data). The fact that the vast majority of ND66 cross-linking products is located in the region of amino acids 83−99 (YKENMGKGTPLPVTPEM, peptides *a*−*d*, Table 1 and Figure 8A) suggests that this region is at or near the molecular interface between ND66 and CaM. It is significant that the interaction site of nebulin and CaM is within 4−20 amino acids of residues 103−107 (KHNQE) in ND66 that have been shown to be cross-linked to actin (in a two-module construct, ND8) (*25*). The proximity of the actin and CaM binding sites on nebulin suggests that CaM weakens the actin−nebulin interaction by competing for neighboring or overlapping sites on nebulin.

The nebulin binding sites on CaM are found at both the lobes and the central helix. It is not clear whether a single nebulin module interacts with all of these sites or if it reflects a montage of sites, each derived from a different complex. The latter possibility is supported by the fact that the 1:1 complexes are resolved to two or three bands on SDS gel, which were analyzed here together as a mixture.

Intramolecular Cross-Linking. Cross-linking between peptides from the same polypeptide provides useful information about its folding in solution, either alone or in a complex with other proteins.

Calmodulin is a dumbbell-shaped protein with a central helix separating two lobes, each of which contains two EF-hands (*27*) that chelate Ca^{2+} ions. The identification of the six intramolecular cross-linking products of CaM indicates that in the course of the cross-linking reaction, these sites

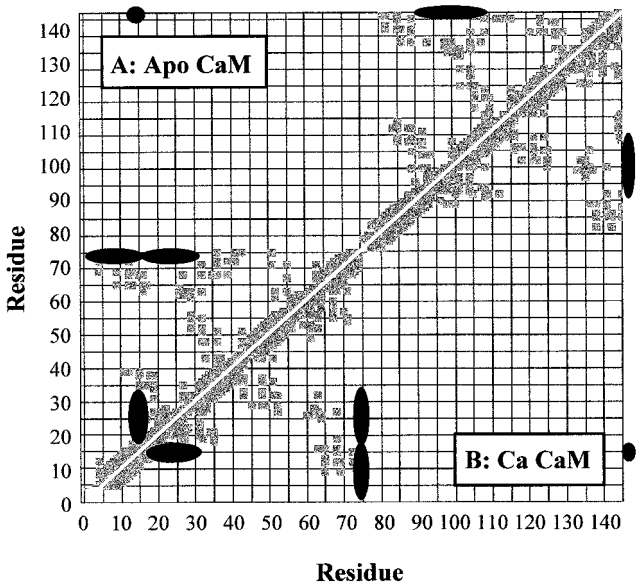

FIGURE 9: Diagonal plots of inter-residue contacts in CaM. The inter-residue contacts of CaM residues in two conformational states are presented as off-diagonal spots above and below the diagonal line of the two-dimensional plots. The contacts based on X-ray crystallography and NMR are represented as squares (from http://structbio.vanderbilt.edu/cabp_database/index.html, with permission), and those determined by our DB cross-linking data are represented as spots superimposed on both contact maps. Note that the size and span of the cross-linking reagents are not represented here. (A) Calcium free CaM (*Xenopus laevis*, NMR solution structure, Protein Data Bank entry 1CFC). (B) Calcium-loaded CaM (*Homo sapiens*, crystal structure at 1.7 Å resolution, Protein Data Bank entry 1CLL).

come within ~6 Å of each other. The two-dimensional plots in Figure 9 are designed to visualize the inter-residue contacts quickly as off-diagonal spots and/or boxes. The overlaying of contact maps from cross-linking with other structural techniques allows "unusual" contacts to be identified with ease. For example, all except one off-diagonal spots overlay with the contacts determined by crystallography and solution NMR (Figure 9). However, the off-diagonal spot near residues ~13−18 to residues 145−148 does not overlay and indicates contact(s) between the two lobes of CaM that was not revealed by either crystallography or NMR. These data suggest that the central helix as well as other parts of CaM may be more flexible and dynamic than the static image conveyed by the crystallographic structure. Indeed, solution studies (*29*−*36*) as well as computational modeling (*37*) indicate that fully Ca^{2+} loaded CaM can adopt conformations more compact than those observed in the crystallographic structure (*28*).

For the four-module fragment ND66, intramolecular cross-linking occurred between residues 1−6 (first module) and residues 114/115−129 (third module), and residues 57 and 58 (second/third module) and residues 83/84−87 (third module). It is worth noting that residues 83−87 are also observed as a site of cross-linking to CaM. This preferential cross-linking of the third module may result from either possible difference of affinity among the four nebulin modules toward CaM and/or the preferential thiolation of the lysines in the third module. Our data thus do not allow us to address the question of whether different modules of ND66 may possess different affinities toward CaM. The intramolecular cross-linking of ND66 provides interesting clues as to how the nebulin modules may interact in solution. The first and fourth module and the second and third module may approach and even contact each other, implying affinity between these nebulin modules. Such intermodule interaction may lead to folding of nebulin peptides into a higher-order structure or to oligomerization. Whether such an interaction manifests itself in the sarcomere, where nebulin is thought to run alongside actin filaments, tropomyosin, and troponin, remains to be established.

In summary, we have shown that chemical cross-linking in conjunction with HPLC and mass spectrometry is potentially capable of providing solid and detailed structural information about molecular interfaces and protein folding that is otherwise not amendable to X-ray crystallography. Further identification of sites in higher-order cross-linked complexes between nebulin, CaM, actin, and myosin is likely to shed new light on the fundamental interactions that underlie or support the calcium-dependent regulatory role of nebulin in skeletal muscle.

ACKNOWLEDGMENT

We thank Dr. Kan Ma for critical reading of the manuscript and valuable suggestions. We thank Wanxia Li and Gustavo Gutierrez-Cruz for preparation of CaM and ND66. We thank Dr. Thomas C. Squier for providing the CaM clone and Dr. Walter J. Chazin for granting permission to use his contact plots in Figure 9.

REFERENCES

1. Allen, J. B., Walberg, M. W., Edwards, M. C., and Elledge, S. J. (1995) *Trends Biochem. Sci. 20*, 511−516.
2. Wang, K., and Richards, F. M. (1975) *J. Biol. Chem. 250*, 6622−6626.
3. Bennett, K. L., Kussmann, M., Björk, P., Godzwon, M., Mikkelsen, M., Sørensen, P., and Roepstorff, P. (2000) *Protein Sci. 9*, 1503−1518.
4. Rappsilber, J., Siniossoglou, S., Hurt, E. C., and Mann, M. (2000) *Anal. Chem. 72*, 267−275.
5. Sinz, A., and Wang, K. (2000) in *Proceedings of the 48th ASMS Conference on Mass Spectrometry and Allied Topics*, Long Beach, CA.
6. Kosower, E. M., and Kosower, N. S. (1995) *Methods Enzymol. 251*, 133−148.
7. Wang, K., and Williamson, C. L. (1980) *Proc. Natl. Acad. Sci. U.S.A. 77*, 3254−3258.
8. Wang, K., and Wright, J. (1988) *J. Cell Biol. 107*, 2199−2212.
9. Kruger, M., Wright, J., and Wang, K. (1991) *J. Cell Biol. 115*, 97−107.
10. Labeit, S., Gibson, T., Lakey, A., Leonard, K., Zeviani, M., Knight, P., Wardale, J., and Trinick, J. (1991) *FEBS Lett. 282*, 313−316.
11. Pelin, K., Hilpela, P., Donner, K., Sewry, C., Akkari, P. A., Wilton, S. D., Wattanasirichaigoon, D., Bang, M. L., Centner, T., Hanefeld, F., Odent, S., Fardeau, M., Urtizberea, J. A., Muntoni, F., Dubowitz, V., Beggs, A. H., Laing, N. G., Labeit, S., de la Chapelle, A., and Wallgren-Pettersson, C. (1999) *Proc. Natl. Acad. Sci. U.S.A. 96*, 2305−2310.
12. Laing, N. G. (1999) *Curr. Opin. Neurol. 12*, 513−518.
13. Fock, U., and Hinssen, H. (1999) *J. Comp. Physiol., B 169*, 555−560.
14. Wright, J., Huang, Q. Q., and Wang, K. (1993) *J. Muscle Res. Cell Motil. 14*, 476−483.
15. Labeit, S., and Kolmerer, B. (1995) *J. Mol. Biol. 248*, 308−315.
16. Wang, K., Knipfer, M., Huang, Q. Q., van Heerden, A., Hsu, L., Gutierrez, G., Quian, X. L., and Stedman, H. (1996) *J. Biol. Chem. 271*, 4304−4314.

17. Pfuhl, M., Winder, S. J., and Pastore, A. (1994) *EMBO J. 13*, 1782−1789.
18. Jin, J. P., and Wang, K. (1991) *J. Biol. Chem. 266*, 21215−21223.
19. Zhang, J. Q., Weisberg, A., and Horowits, R. (1998) *Biophys. J. 74*, 349−359.
20. Gonsior, S. M., Gautel, M., and Hinssen, H. (1998) *J. Muscle Res. Cell Motil. 19*, 225−235.
21. Root, D. D., and Wang, K. (1994) *Biochemistry 33*, 12581−12591.
22. Strasburg, G. M., Hogan, M., Birmachu, W., Thomas, D. D., and Louis, C. F. (1988) *J. Biol. Chem. 263*, 542−548.
23. Hühmer, A. F., Aced, G. I., Perkins, M. D., Gursoy, R. N., Jois, D. S., Larive, C., Siahaan, T. J., and Schöneich, C. (1997) *Anal. Chem. 69*, 29R−57R.
24. Huang, Q. Q. (1993) Monoclonal antibodies against cloned human nebulin fragments, Master's Thesis, University of Texas at Austin, Austin, TX.
25. Shih, C. L., Chen, M. G., Linse, K., and Wang, K. (1997) *Biochemistry 36*, 1814−1825.
26. O'Neil, K. T., and DeGrado, W. F. (1990) *Trends Biochem. Sci. 15*, 59−64.
27. Kretsinger, R. H., and Nockolds, C. E. (1973) *J. Biol. Chem. 248*, 3313−3326.
28. Babu, Y. S., Bugg, C. E., and Cook, W. J. (1988) *J. Mol. Biol. 204*, 191−204.
29. Heidorn, D. B., and Trewhella, J. (1988) *Biochemistry 27*, 909−915.
30. Persechini, A., and Kretsinger, R. H. (1988) *J. Cardiovasc. Pharmacol. 12* (Suppl. 5), S1−S12.
31. Small, E. W., and Anderson, S. R. (1988) *Biochemistry 27*, 419−428.
32. Török, K., Lane, A. N., Martin, S. R., Janot, J. M., and Bayley, P. M. (1992) *Biochemistry 31*, 3452−3462.
33. Yao, Y., Schöneich, C., and Squier, T. C. (1994) *Biochemistry 33*, 7797−7810.
34. Persechini, A., Jarrett, H. W., Kosk-Kosicka, D., Krinks, M. H., and Lee, H. G. (1993) *Biochim. Biophys. Acta 1163*, 309−314.
35. Yao, Y., and Squier, T. C. (1996) *Biochemistry 35*, 6815−6827.
36. Sun, H., Yin, D., and Squier, T. C. (1999) *Biochemistry 38*, 12266−12279.
37. Pascual-Ahuir, J. L., Mehler, E. L., and Weinstein, H. (1991) *Mol. Eng. 1*, 231−247.
38. Biemann, K. (1990) *Methods Enzymol. 193*, 886−887.

BI010259+